HHS Public Access

Author manuscript

J Immunol. Author manuscript; available in PMC 2017 February 15.

Published in final edited form as:

J Immunol. 2016 February 15; 196(4): 1495–1506. doi:10.4049/jimmunol.1403251.

Loss of peripheral protection in pancreatic islets by proteolysis-driven impairment of VTCN1 (B7-H4) presentation is associated with the development of autoimmune diabetes

Ilian A. Radichev[*], **Lilia V. Maneva-Radicheva**[*], **Christina Amatya**[*], **Maryam Salehi**[*], **Camille Parker**[*], **Jacob Ellefson**[*], **Paul Burn**[*], and **Alexei Y. Savinov**[*,†]

[*]Sanford Project/Children's Health Research Center, Sanford Research, Sioux Falls, South Dakota, USA

[†]Department of Pediatrics, University of South Dakota School of Medicine, Sioux Falls, South Dakota, USA

Abstract

Antigen-specific activation of T cells is an essential process in the control of effector immune responses. Defects in T cell activation, particularly in the co-stimulation step, have been associated with many autoimmune conditions including type 1 diabetes (T1D). Recently, we demonstrated that the phenotype of impaired negative co-stimulation, due to reduced levels of V-set domain-containing T cell activation inhibitor-1 (VTCN1) protein on antigen-presenting cells, is shared between diabetes-susceptible NOD mice and human T1D patients. Here, we show that a similar process takes place in the target organ, as both α and β cells within pancreatic islets gradually lose their VTCN1 protein during autoimmune diabetes development despite the up-regulation of the *VTCN1* gene. Diminishment of functional islet cells' VTCN1 is caused by the active proteolysis by metalloproteinase NRD1 and leads to the significant induction of proliferation and cytokine production by diabetogenic T cells. Inhibition of NRD1 activity, on the other hand, stabilizes VTCN1 and dulls the anti-islet T cell responses. Therefore, we suggest a general endogenous mechanism of defective VTCN1 negative co-stimulation, which affects both lymphoid and peripheral target tissues during T1D progression and results in aggressive anti-islet T cell responses. This mechanism is tied to up-regulation of *NRD1* expression and likely acts in two synergistic proteolytic modes: cell-intrinsic intracellular and cell-extrinsic systemic. Our results highlight an importance of VTCN1 stabilization on cell surfaces for the restoration of altered balance of immune control during T1D.

Introduction

Type 1 diabetes (T1D) is a life-threatening disease of autoimmune nature, for which the only currently available treatment is continuous insulin administration. Clinical T1D arises as a consequence of the cytotoxic destruction of insulin-producing β cells by abnormally activated autoreactive T cells specific for multiple islet cells' antigens (1, 2). Accumulating

Corresponding author: Dr. Alexei Savinov, Sanford Project/Children's Health Research Center, Sanford Research, 2310 East 60th Street North, Sioux Falls, SD, 57104, USA, Phone: (605) 312-6019; Fax: (605) 312-6071; Alexei.Savinov@sanfordhealth.org.

evidence, however, suggests that islet cells do not merely play a role of plain targets of autoimmune destruction, but on contrary, possess several protective mechanisms capable of down-regulation of autoimmune attack (3, 4). One of such mechanisms is at the center of our investigation.

V-set domain-containing T cell activation inhibitor-1 (VTCN1), also known as B7-H4, B7S1, B7X, is a negative co-stimulatory molecule; one of the newly discovered members of B7 family (5-7). VTCN1 acts through a not yet identified receptor on T cells, inhibiting T cell activation, proliferation, and cytokine production (5, 6, 8, 9). The persistence of autoreactive T cell responses during T1D prompted several experimental attempts to alleviate diabetogenic autoimmunity *via* artificial enrichment of VTCN1-mediated co-inhibition. Accordingly, matrix-surface-bound VTCN1-Ig fusion protein suppressed the proliferation of islet-specific T cell clones derived from T1D patients. Furthermore, the treatment of diabetes-susceptible non-obese diabetic (NOD) mice with VTCN1-Ig protein significantly attenuated T1D (10).

Unlike classical co-stimulatory molecules (B7-1 and B7-2), whose natural expression and action is strictly limited to antigen-presenting cells (APCs) (11, 12), VTCN1 is also expressed in several non-lymphoid organs, and most importantly, in pancreatic islets (6, 7, 9, 13-15). Consequently, VTCN1 has been hypothesized to not only inhibit classical T cell activation by APCs in the lymphoid compartment, but also induce T cell tolerance within peripheral target tissues. Supporting this suggestion, up-regulated *VTCN1* expression was detected in multiple neoplasms (7, 13, 16-18), where it was associated with tumor-protective down-regulation of anti-tumor T cell responses (19).

In T1D setting, transfection of *VTCN1-Ig* construct into human primary islet cells protected them from diabetogenic T cell clones isolated from T1D patients (14). Additionally, *ex vivo VTCN1* over-expression in mouse islets shielded them from T cell-induced damage in transplantation experiments (20), while *in vivo* β-cell-specific *VTCN1* over-expression protected against diabetes induced by both $CD4^+$ and $CD8^+$ islet-specific clonal T cells (9, 21). Therefore, the distinctive combination of T cell co-inhibitory function with expression on islet cells uniquely positions VTCN1 at the interface of pancreatic islets and the immune system.

Despite the growing number of functional studies utilizing genetically manipulated VTCN1 (overexpression and/or deletion), the state of natural VTCN1 on either APCs or islet cells in connection with T1D development is largely unknown. That is why we asked the question of whether or not a compromised function of endogenous VTCN1 can trigger enhanced vulnerability of islet tissue to diabetogenic autoimmunity. Recently, we unveiled an endogenous pathway of functional VTCN1 inactivation in APCs (particularly in macrophages – MΦs, and dendritic cells – DCs) of NOD mice and T1D patients. Specifically, a gradual loss of membrane-tethered VTCN1 due to a proteolytic cleavage mediated by metalloproteinase nardilysin (NRD1), progressed alongside natural T1D development, and triggered hyper-proliferation of diabetogenic T cells (22). Here, we extend our previous findings and dissect a pattern of VTCN1 expression and presentation on islet cells in connection with diabetogenesis. Subsequently, we define a general mechanism of a

progressive loss of VTCN1-mediated negative co-stimulation, which occurs in multiple tissues/cells (islet endocrine cells and APCs) due to the NRD1-dependent diminishment of membrane VTCN1. This mechanism is linked to T1D susceptibility, and depends on two separate but synergistic processes. First is a result of an increased intracellular NRD1 expression, ultimately leading to enhanced intracellular VTCN1 shedding. The second process includes a systemic up-regulation of *NRD1* (an enzyme with both intra- and extra-cellular activities) (23, 24) in multiple tissues, which additionally potentiates VTCN1 proteolysis by extracellular NRD1. In summary, our findings point toward VTCN1 stabilization along with systemic NRD1 inhibition as future strategies for T1D treatment.

Materials and Methods

Chemicals

All chemicals were from Fisher Scientific (Suwanee), unless stated otherwise. 1,10-Phenanthroline, Bestatin, Collagenase P and Histopaque were from Sigma-Aldrich (St. Louis).

Human subjects

Postmortem pancreatic tissue samples from diabetic and control donors were obtained from South Dakota Lions Eye & Tissue Bank.

Mice

NOD/ShiLtJ (NOD), NOD.CB17-*Prkdc*^{scid}/J (NOD-*scid*), NOD.Cg-*Prkd*^{cscid} Tg(CAG-EGFP)10sb/KupwJ (NOD-*scid*-EGFP), NOD.Cg-Rag1^{tm1Mom}Tg(TcraBDC12-4.1) 10JosTg(TcrbBDC12-4.1)82Gse/J (NOD.BDC12-4.1), B6.129S7-Rag1^{tm1Mom}/J (B6-Rag1$^{-/-}$), and B6.NOD-(D17Mit21-D17Mit10)/LtJ (B6^{g7}) mice were purchased from The Jackson Laboratory. B6.G9C8 mice, transgenic for TCR derived from insulin-specific CD8^{+} T cell clone G9C8, and *H-2K*^{d} MHC allele (25) were a kind gift by Dr. A. Chervonsky (University of Chicago). B6.NOD-(D17Mit21-D17Mit10)-Rag1^{tm1Mom} (B6^{g7}-Rag1$^{-/-}$) mice where generated by crossing B6-Rag1$^{-/-}$ with B6^{g7}, then intercrossing F1 animals to produce F2 population, which was typed by FACS for presence of T cells in peripheral blood and by PCR for presence of *H-2*^{g7} using 5′-TGCACTTGCATAAGGAAAAC-3′ and 5′-GACTTTGGGGCCTACTTATG-3′ as forward and reverse primers, respectively. Only both *H-2*^{g7}-positive and T cells-negative mice were used. To generate bone marrow (BM) chimeric mice B6^{g7} or EGFP-positive (NOD × NOD-*scid*-EGFP) F1 (NOD-EGFP) were used as either BM donors or recipients. All mice were maintained in the Sanford Research Animal Facility according to the NIH guidelines for animal use.

In vivo bestatin treatments

Female NOD mice at six weeks of age were injected daily (*i.p.*) with either vehicle or 10 mg/kg bestatin (Fig. 3A). Two groups (n=7/group) were treated for four weeks, the other two (n=12-14/group) - until diabetes development. To analyze the proliferation of insulitis-forming cells, all animals in the four weeks treatment groups received *i.p.* injections of 2.5 mg/kg EdU for the last four consecutive days of treatments. Mice were then euthanized and MΦs, pancreatic lymph nodes (PLN), spleens and pancreata were collected for analysis.

From 12 weeks of age all mice were monitored daily for urine glucose using Diastix strips (Diastix). Mice with the urine glucose ≥250 mg/dL on two consecutive days were confirmed diabetic by a blood glucose analysis and euthanized. MΦs were collected from diabetic mice.

Adoptive transfers and generation of bone marrow chimeras

Adoptive transfers were performed by *i.v.* injection of 10^7 splenocytes from diabetic NOD into irradiated (600 Rads) $B6^{g7}$ or non-irradiated $B6^{g7}$-*Rag1*$^{-/-}$ or NOD-*scid* recipients as previously described (26). Sham-transferred mice were not irradiated and received PBS. Starting from day 18 post-transfer, recipient mice were injected *i.p.* for four consecutive days with 2.5 mg/kg of EdU per day. Mice were then sacrificed and pancreatic cryosections were prepared.

To generate chimeric mice, lethally irradiated (950 Rads) 6 – 7 week-old female recipients were injected *i.v.* with 1×10^7 of BM cells, isolated from tibias and femurs of donor mice as previously described (27). NOD-EGFP mice were used to distinguish between recipient's and donor's cells in the chimeric animals. To confirm the chimerism, recipients' PBMCs were analyzed 3 and 10 weeks after BM transfers for EGFP-positivity by FACS. Mice were euthanized 10 weeks post BM transplantations. Peritoneal MΦs and pancreata were collected for further analyses.

Isolation of macrophages

Thioglycollate-elicited mouse peritoneal MΦs (for the co-culturing experiments and from $B6^{g7}$/NOD chimeras) or peritoneal cavity-residential MΦs (from bestatin-treated mice) were collected in PBS and plated for immunofluorescence (onto coverslips) or RNA isolation (in 6-well plate). Only the adherent cells were then used for analyses.

Isolation and culture of mouse pancreatic islets

Islets were isolated by collagenase digestion as described (28). Handpicked islets (n>50) were then either lysed in 1 ml TRIzol (Life Technologies) for isolation of RNA, or dispersed for islet cells/T cells co-cultures. Undispersed islets were cultured to either condition medium or for *in vitro* treatments. The effects of NRD1 inhibitors were evaluated after in-culture treatments of freshly-isolated whole islets for 24 h with either bestatin (10 μM), or phenanthroline (20 μM), or vehicle solution. The islets were then fixed with ice-cold methanol and VTCN1 levels were analyzed by immunofluorescence. To prepare conditioned medium, islets (>20 per well) were cultured in 48-well plate for 16 h in 200 μl serum-free RPMI.

T cells - islet cells co-cultures

For *in vitro* T cells activation assays, isolated islets were dispersed into single-cell suspensions in cell-dissociation buffer (Life Technologies) for 15 min at 37°C. Dispersed islet cells were then washed, depleted from plastic and nylon wool-adherent APCs for 1 h at 37°C, and incubated for 24 h in 96-well plates with RPMI medium containing 10% FBS in the presence or absence of 10 μM bestatin.

G9C8 or BDC 12-4.1 T cells were isolated from spleens of B6.G9C8 or NOD.BDC12-4.1 mice respectively, *via* mechanical disruption of spleens followed by the lysis of red blood cells. In some experiments G9C8 T cells were purified from bulk spleen population using Pan T cells Purification Kit II (Miltenyi Biotec). Isolated T cells were then labeled with carboxyfluorescein diacetate succinimidyl ester (CFSE) (Life Technologies) and 1×10^5 cells were added to the cultures of dispersed islets containing either bestatin or vehicle solution. In some experiments, 2×10^4 of NOD peritoneal MΦs were incubated with disrupted islets for 24 h in presence of either bestatin or vehicle solution before addition of BDC12-4.1 T cells. After five days of co-cultures, the non-adherent cells were collected, washed, and analyzed by Flow cytometry for CFSE dilution. On day 3, 100 μl of conditioned medium was collected for IL-2 ELISA analysis, and then fresh medium with 5U/ml of recombinant IL-2 (BioLegend) was added to the co-cultures. Non-specific activation of G9C8 T cells with anti-CD3/anti-CD28-coated beads (ThermoFisher Scientific) in presence/absence of bestatin was carried out for 5 days in the same experimental conditions as co-cultures.

ELISA

IL-2 concentrations were analyzed using Mouse IL-2 Platinum ELISA kit (eBioscience) following manufacturer's recommendations.

Immunofluorescence and histological analyses

Frozen in O.C.T. compound, pancreata were cryosectioned into 5 μm-thick sections and placed on Superfrost glass slides. Slides were fixed in 100% Acetone at -20°C, air-dried, and then stored at -80°C before processing. Cryosections were stained with either goat anti-mouse VTCN1 (2 μg/ml; R&D Systems) or mouse anti-human VTCN1 (5 μg/ml; eBioscience) and then visualized with the respective secondary AlexaFluor-488 conjugated donkey anti-goat or donkey anti-mouse antibodies (Jackson Immunoresearch). Pancreatic β and α cells were stained with guinea-pig anti-insulin (1:100) and rabbit anti-glucagon (1:100), respectively (both from Abcam), followed by the corresponding secondary donkey antibodies conjugated either with AlexaFluor-594 or AlexaFluor-647 (Jackson Immunoresearch). For staining of MΦs, rat anti-mouse F4/80 (5 μg/ml) (eBioscience) was used. Peritoneal MΦs were fixed in 4% PFA and then stained with rat anti-mouse VTCN1 (5 μg/ml; R&D Systems) followed by donkey anti-rat conjugated with AlexaFluor-594 (Jackson Immunoresearch). Pancreatic sections from animals injected with EdU were stained for insulin and CD3, and assessed for T cell proliferation *via* detection of EdU incorporation into the DNA of replicating cells, as previously described (29). CD3-positive cells in the insulitis area were counted and the percentage of EdU positive cells was calculated. More than 130 islets with over 30,000 infiltrating cells per group were analyzed.

To analyze insulitis, pancreatic sections were stained for insulin and islet infiltration was graded in a blinded fashion from 0 (intact islets) to 4 (virtually no β cells within the islet infiltrate) and then divided into three sub-categories: 1) “no insulitis” – islets with grade 0; 2) “mild insulitis” – islets with grades 1 and 2; and 3) “severe insulitis” – islets with grades 3 and 4. The percentage of islets falling into each sub-category was calculated for each experimental group.

All images were acquired on Nikon's A1 confocal microscope. Imaging conditions were kept constant for all samples within an experiment. Results were expressed as relative fluorescent units (RFU) of VTCN1 staining calculated from at least 100 individual cells or >30 islets.

RNA isolation and cDNA generation

Total RNA was purified from MΦs or pancreatic islets using Direct-zol RNA MiniPrep kit (Zymo Research) from samples collected in TRIzol. Only RNAs with RIN number higher than 8.0 were used for generation of cDNA and subsequent RT-qPCR analysis. cDNA was generated using GoScript Reverse Transcription System (Promega).

RT-qPCR

RT-qPCR analysis using primers specific for *VTCN1*, *NRD1*, *PCSK1*, or *PCSK2* was performed as previously described (22).

Flow Cytometry analysis (FACS)

All antibodies were purchased from eBioscience (San Diego), unless stated otherwise. To analyze T regulatory cells (Tregs), single cell suspensions from spleens and PLN were blocked with 10 μg/ml anti-mouse CD16/CD32, then incubated for 30 min with 2.5 μg/ml anti-CD4-FITC and 2 μg/ml anti-CD25-APC. The cells were then washed, incubated in Fixation/Permeabilization buffer and stained for 30 min with 5 μg/ml PE-conjugated anti-FoxP3 antibody.

Analysis of diabetogenic NRP-V7- mimitop-reactive $CD8^+$ cells was performed in splenocytes and PLN cells that were consequently incubated with 10 μg/ml PE-conjugated H-$2K^d$-KYNKANVFL pentamer (ProImmune) and 2.5 μg/ml FITC-conjugated anti-CD8 for 10 and 30 min, respectively. Cells were then washed and stained with the TO-PRO-3 (Life Technologies) viability marker. The viability marker 7AAD (7-amino-actinomycin D; 0.5 μg/ml) (eBioscience) was used to detect the dead cells during analyses of *in vitro* activated G9C8 or BDC12-4.1 T cells and in PBMSs collected from chimeric mice. For analysis of co-cultured BDC12-4.1 T cells proliferation, the cells were also stained for 1 h with 5 μg/ml APC-conjugated anti-CD69 (BioLegend). Samples were then recorded on an Accuri C6 cytometer (BD Biosciences) and analyzed with FlowJo software (Tree Star). All gating strategies are shown as supplemental material (Fig. S3 and Fig. S4).

Immunoblot analysis

Serum-free medium was conditioned by pancreatic islets for 24 h at 37°C. Cell lysates were prepared in RIPA buffer as described before (22). The samples (5 μg total protein) were subjected to electrophoresis through a 4 – 12% NuPAGE Bis-Tris polyacrylamide gel. The membranes were blocked with C-PBST (1% Casein, 0.1% Tween-20 in PBS) and probed with goat anti-VTCN1 (LifeSpan Biosciences) or rabbit anti-NRD1 (Proteintech). HRP-conjugated anti-goat or anti-rabbit (1:5,000) (Jackson Immunoresearch) were the secondary antibodies followed by chemiluminescent substrate (Super Signal West Dura Substrate, Pierce). The membranes were then scanned on a UVP Biospectrum 500 imaging system.

Statistical analysis

Statistical analysis was performed using GraphPad Prism 6 (GraphPad Software). Differences in T1D incidence rates were assessed using Log-rank survival curve analysis. Differences in pair-wise comparisons between groups were assessed using two-tailed Student's t test with a significance threshold of $p \leq 0.05$.

Results

Proteolytic loss of endogenous VTCN1 from pancreatic islets progresses alongside T1D development

In order to investigate whether presentation of endogenous VTCN1 by islet cells can be tied to the development of diabetogenic autoimmunity, we compared the dynamics of VTCN1 levels in Langerhans' islets in diabetes-susceptible NOD and diabetes-resistant $B6^{g7}$ mice. Immunofluorescent staining of pancreatic sections revealed an age-dependent progressive loss of VTCN1 protein from NOD islets (Fig. 1A, *left panel*). Such loss became noticeable around 9 – 10 weeks of age and led to widespread decline of VTCN1 by 15 weeks of age, which is the average time of T1D onset in our NOD colony. Conversely, $B6^{g7}$ animals had stable intra-islet VTCN1 levels throughout observation time. The analysis of mean fluorescent intensities confirmed a statistically significant decrease of VTCN1 signal in NOD *vs.* $B6^{g7}$ islets (Fig. 1A, *right panel*).

VTCN1 mRNA, however, increased with age in islets of diabetes-prone NOD animals, while an opposite non-significant trend towards age-dependent down-regulation of *VTCN1* expression characterized the $B6^{g7}$ islets (Fig. 1B). The augmentation of *VTCN1* gene expression was even more evident and, importantly, was paralleled by the significant increase in metalloproteinase *NRD1* gene expression when islets from pre-diabetic NOD mice were directly compared to the ones from age-matched $B6^{g7}$ animals (Fig. 1C). These findings echoed our recent report describing a highly similar phenotype of progressive VTCN1 protein loss (coupled with compensatory *VTCN1* mRNA up-regulation) in MΦs and DCs from T1D-succeptible subjects, which occurred due to proteolysis of cell-associated VTCN1 by the metalloproteinase NRD1 (22). Hence, we compared dynamics of islet *NRD1* expression and observed a significant age-dependent elevation of *NRD1* mRNA in NOD, but not $B6^{g7}$ islets (Fig. 1D). Accordingly, levels of NRD1 proteinase were also augmented in pre-diabetic NOD islets in comparison to age-matched $B6^{g7}$ (Fig. 1E). Moreover, the amounts of intracellular NRD1 enzyme increased in NOD islets with age, paralleling T1D progression. To confirm that proteolytic shedding is indeed the mechanism liable for the observed VTCN1 decline, we cultured freshly-isolated NOD and $B6^{g7}$ islets and detected elevated levels of soluble VTCN1 immunogenic fragments in medium conditioned by islets of pre-diabetic NOD mice (Fig. 1F).

To characterize VTCN1 expression in different types of pancreatic endocrine cells and to examine whether VTCN1 loss observed in islets of T1D-succeptible mice extends to human T1D patients, we analyzed pancreatic sections immunostained for VTCN1, insulin, and glucagon. In human subjects, both glucagon-expressing α cells and insulin-expressing β cells were VTCN1-positive (Fig. S1A), although the VTCN1 signal was generally higher in

α cells. Likewise, in murine islets both α and β cells expressed VTCN1 (Fig. S1B), however, contrary to humans, VTCN1 immunoreactivity in β cells was considerably stronger than in α cells. Evaluation of VTCN1 immunofluorescence in islets from a small cohort of T1D patients revealed, that similarly to NOD mice, the islet remnants from a representative T1D donor displayed substantially reduced VTCN1 levels relative to islets from a representative healthy subject (Fig. S1C). Interestingly, a small number of undersized islets in the T1D patient were strongly positive for both insulin and VTCN1 (Fig. S1D).

Taken together, these results suggest that proteolytic loss of VTCN1 in multiple islet cells accompanies the course of T1D development in both humans and mice.

Inhibition of NRD1-mediated VTCN1 proteolysis in islets alters diabetogenic T cell responses

Besides NRD1, pancreatic endocrine cells express two functional proprotein convertases: PCSK1 and PCSK2, which, by *in silico* analysis using Eukaryotic Linear Motif database (http://elm.eu.org/), are predicted to target VTCN1 cleavage. Hence, we compared mRNAs expression of these enzymes as well as of PCSK1 Inhibitor (*PCSK-1N*) in islets isolated from NOD and $B6^{g7}$ mice. A non-significant trend toward up-regulation of all these molecules was found in NOD islets (Fig. S2). Therefore, to ratify that the proteolytic clearance of VTCN1 from pancreatic islets is mediated by NRD1, we used two inhibitors known to inhibit NRD1, but not PCSK1 or PCSK2: 1,-10-phenanthroline and bestatin (30-32) for *ex vivo* in-culture treatments of non-dispersed “VTCN1-low” islets freshly isolated from 13-15 week-old NOD mice. Both inhibitors stabilized islet-associated VTCN1, as confirmed by the increase of VTCN1 immunofluorescence (Fig. 2A), thus, implying that NRD1 is indeed the mediator of VTCN1 shedding from islet cells. Similar *ex-vivo* bestatin treatment of “VTCN1-high” islets from 6 week-old either $B6^{g7}$ or NOD mice did not change islets' VTCN1 levels in all animals analyzed (not shown).

Next, we examined the functional impact of NRD1 inhibitor-induced VTCN1 conservation for down-regulation of anti-islet immune responses. For that, dispersed to single cells “VTCN1-low” islets from 13 weeks-old NOD mice were pre-treated with either bestatin, or vehicle for 24 hours, then co-cultured for 5 days (with inhibitor still present) with CFSE-labeled either bulk spleen cells, or purified T cells from B6.G9C8 mice. B6.G9C8 animals express rearranged α and β chains of TCR from insulin B chain (a.a.15-23)-specific $CD8^+$ T cell clone G9C8, and also its MHC $H\text{-}2K^d$ restriction allele (25). Therefore, these mice are an excellent source of diabetogenic $CD8^+$ T cells of a single G9C8 clonotype, which are capable of the direct β cells recognition (33). While purification decreased the absolute numbers of dividing G9C8 T cells, the overall proliferative behavior of purified T cells in inhibitor-treated co-cultures with islet cells (not shown) was very similar to that of the bulk G9C8 cells, which are illustrated on Figure 2 B and C. Specifically, bestatin-treated islet cells prompted a statistically significant reduction of proliferative capacity of co-cultured G9C8 T cells when compared to vehicle-treated islets (Fig. 2B). Moreover, the production of the pro-proliferative cytokine IL-2 by G9C8 cells co-cultured with bestatin-treated islets was also decreased (Fig. 2C). To control for the possibility that the decline in G9C8 T cell propagation is due to a direct anti-proliferative effect(s) of bestatin, rather than the

consequence of bestatin-induced VTCN1 preservation, we used antigen-independent activation of G9C8 cells by anti-CD3/CD28 beads. The presence of bestatin in these control reactions did not affect the propagation of G9C8 cells (Fig. 2B), indicating that stabilization of endogenous VTCN1 in islet cells and, in particular, in β cells, *via* NRD1 inhibition, directly reduces proliferation of diabetogenic $CD8^+$ T cells.

Previously we reported that proteolysis-dependent decrease of VTCN1 levels on APCs from diabetes-prone NOD mice potentiates *in vitro* hyper-activation and proliferation of autoreactive T cells (22). In order to reveal whether such mechanism contributes to the peripheral tolerance mediated by islet-resident APCs, cross-presenting β cells antigens to diabetogenic $CD4^+$ T cells, we used CFSE-labeled splenocytes isolated from NOD.BDC12-4.1 mice in our co-culture experiments. NOD.BDC12-4.1 mice bear Rag1 recombinase deficiency coupled with the transgenic expression of both α and β chains of TCR from highly pathogenic AI^{g7}-restricted insulin B chain (a.a. 9-23)-reactive $CD4^+$ T cell clone (34). Analysis of BDC12-4.1 cells co-cultured, as described above, with bestatin- or vehicle-treated suspensions of islet cells from 13 week-old NOD mice revealed a significant bestatin-induced reduction in proliferative rates of BDC12-4.1 T cells (Fig. 2D). The increase of APCs load (*via* addition of exogenous “VTCN1-low” peritoneal MΦs from 17 week-old NOD mice) in these conditions markedly augmented proliferative responses of BDC12-4.1 T cells, while the significant bestatin-mediated reduction of BDC12-4.1 cells proliferation was kept intact (Fig. 2D).

In sum, these results suggest that bestatin-induced NRD1 inhibition stabilizes VTCN1 on multiple types of islet cells (in particular, islet-resident APCs and β cells), which co-contribute to the peripheral tolerance *via* down-regulation of anti-islet T cells responses.

Continuous *in vivo* administration of NRD1 inhibitor delays diabetes in NOD mice

To test whether the systemic NRD1 inhibition *in vivo* will alleviate VTCN1 loss on the islet cells and peripheral APCs and, consequently, alter the course of diabetes, six week-old NOD female mice were injected (*i.p.*) daily with 10 mg/kg of bestatin (Fig. 3A). Administration of bestatin moderately but significantly delayed (by three weeks, on average) the onset of disease (Fig. 3B, *left*) and produced significant stabilization of VTCN1 levels on peritoneal MΦs. Interestingly, this effect was much more prominent early in the treatment course (four weeks of administration, 10 weeks of age) than at the latest time points (diabetic animals) (Fig. 3B, *right*). Similarly to the peritoneal MΦs, VTCN1 levels on the islets of mice treated for 4 weeks with bestatin showed a trend towards stabilization, even though this effect did not reach the threshold of statistical significance (Fig 3C *left panel*, p=0.1). Such “incomplete” islets' phenotype is, most likely, the consequence of the intra-peritoneal route of bestatin delivery, which produced higher bestatin concentrations affecting peritoneal MΦs and lower intra-islet concentrations. On the other hand, even partial islets' VTCN1 stabilization in bestatin-treated mice coincided with the significant decrease in numbers of proliferating cells within islets infiltrates, as well as with the significant delay in insulitis formation (Fig. 3C, *middle* and *right* panels), pointing toward partial activation of peripheral tolerance within the islets.

Finally, the analysis of T cell populations in spleens and PLNs of bestatin-treated (4 weeks of treatment) animals revealed that while inhibitor did not affect the relative sizes of both $CD4^+$ and $CD8^+$ T cell populations, it produced a significant elevation of splenic Tregs, as well as a statistically significant decrease in numbers of highly diabetogenic NRP-V7 mimitop-specific $CD8^+$ T cells (35) (Fig. 3D). These later observations mimic the earlier reported effects of VTCN1-Ig treatments of autoimmune mice (10, 36) and thus, validate VTCN1-stabilizing, self-tolerance promoting effects of systemic bestatin administration.

Endogenous VTCN1 shields pancreatic islets by alleviating proliferation of infiltrating T cells

As infiltration of multiple immune cells into peri-islet vicinity (insulitis) is the major T1D trait in both mice and humans (37-39) we assessed whether the loss of VTCN1 from islet cells is induced by insulitis formation or, on contrary, precedes and even potentiates it. For this, we adoptively transferred splenocytes from acutely diabetic NOD mice into 15-20 week-old $B6^{g7}$ recipients, allowed 20 days for islet infiltrates to progress, and then evaluated VTCN1 levels in recipients' islets. Despite the formation of massive peri-islet infiltrates, recipient $B6^{g7}$ mice maintained stable islet VTCN1 levels, which did not differ from the ones observed in the islets of sham-transferred mice (Fig. 4A), implying that insulitis does not induce VTCN1 decline.

Approaching the paradigm of connection between VTCN1 loss and insulitic inflammation from an opposite angle, we analyzed VTCN1 immunofluorescence in islets of NOD-*scid* mice, which have diabetes-susceptible NOD genetic background, but lack autoimmunity due to the $Prkdc^{scid}$ mutation-caused absence of functional T and B lymphocytes (40). Similarly to NOD mice, islets from NOD-*scid* animals displayed progressive age-dependent loss of VTCN1 (Fig. 4B), suggesting that diabetes-prone NOD background predisposes for such loss independently of lymphocytes signaling.

These results raised the important functional question: What are the islet-shielding effects of endogenous VTCN1 presented by islet cells *in vivo*? Since by 15 weeks of age $B6^{g7}$ and NOD-*scid* mice display “high” and “low” VTCN1 levels on their islets, respectively (Fig. 4C), we used 17 – 20 week-old animals of these strains as recipients of adoptive transfers of NOD splenocytes. The VTCN1 levels on recipients' islets were examined 3 weeks after the transfers. Formation of insulitic lesions did not influence VTCN1 levels, which remained stably “high” in $B6^{g7}$ and stably “low” in NOD-*scid* recipient mice (Fig. 4C). We then evaluated the T cell proliferation within the insulitis area of adoptively transferred mice. For these experiments 15 week-old NOD-*scid* recipients were compared to $B6^{g7}$-$Rag1^{-/-}$ mice which, similarly to $B6^{g7}$ animals, maintain “high” VTCN1 levels on islets (not shown) and are lymphopenic equally to NOD-*scid*. The latter is important to eliminate the influence of lymphopenic environment on homeostatic proliferation of transferred cells. The percentage of dividing CD3-positive T cells within peri-islet infiltrates was significantly higher in NOD-*scid* recipient mice, correlating with their lower islet-associated VTCN1 levels (Fig. 4D). Moreover, the percentage of insulitis-free islets in $B6^{g7}$-$Rag1^{-/-}$ mice was significantly higher when compared to NOD-*scid* mice (Fig. 4D *right panel*). Therefore, VTCN1 on islet cells may function as an endogenous protective molecule, which attenuates proliferation of

autoreactive islet-infiltrating T cells, shielding the pancreatic islets from diabetogenic autoimmunity.

VTCN1 levels in multiple cell types are compromised on diabetes-prone NOD background by a general mechanism combining cell-autonomous and systemic *NRD1* up-regulation

Since mice of NOD background succumb to the progressive NRD1-mediated loss of islet-protective VTCN1, we explored a possibility to interfere with such loss. Accordingly, we asked whether stable introduction of B6^{g7}-originated myeloid cells, which display low internal NRD1 and steady VTCN1 levels (22), will be able to prevent and/or delay loss of VTCN1 from NOD islets. For this, we constructed chimeric mice by transplanting bone marrow from B6^{g7} donors into lethally irradiated NOD-EGFP recipients (B6^{g7}→NOD-EGFP). Reciprocal BM transfers from NOD-EGFP mice into B6^{g7} recipients (NOD-EGFP→B6^{g7}), as well as control B6^{g7}→B6^{g7} and NOD-EGFP→NOD BM transplantations were also performed. At the time of the transfers, all recipient mice were 6 – 7 weeks of age, which is before the start of noticeable VTCN1 loss. While it is impossible to assess the effects of lethal irradiation on islets' VTCN1 levels, sub-lethal irradiation doses used in our adoptive transfer experiments did not affect neither progressive loss of islet VTCN1 in NOD mice (not shown), nor the stable islet-tethered VTCN1 levels in B6g7 animals (Fig. 4C). Ten weeks after the BM transplantations, more than 90% of PBMCs in chimeric mice were of the donor's origin (Fig. S3). Stable engraftment of B6^{g7} BM did not alleviate VTCN1 shedding in NOD islets, as VTCN1 immunofluorescence in B6^{g7}→NOD-EGFP chimeras was not significantly different from NOD-EGFP→NOD animals (Fig. 5A). This indicated that VTCN1 loss is predominantly an islet cell-autonomous process intrinsic for NOD islets. NOD-EGFP→B6^{g7} chimeric mice, however, exhibited islet VTCN1 levels significantly lower than B6^{g7}→B6^{g7} chimeras, but nevertheless, significantly higher than NOD-EGFP→NOD chimeric animals (Fig. 5A). This suggests that a long-term introduction of NOD-originated hematopoietic cells can induce partial destabilization of islet VTCN1 in B6^{g7} animals through an extrinsic (islet non-autonomous) mechanism.

To investigate in more details the nature of the systemic VTCN1-ablating stimuli produced by NOD BM-derived cells, we analyzed the phenotype of peritoneal MΦs isolated from the constructed chimeric animals. In agreement with our previous findings demonstrating massive VTCN1 shedding in APCs of diabetes-prone NOD mice (22), NOD BM-originated MΦs exhibited a significant VTCN1 decrease independently from the host's environment that they developed and resided in (NOD-EGFP→B6^{g7} and NOD-EGFP→NOD chimeras *vs.* B6^{g7}→B6^{g7} mice, Fig. 5B), confirming the inherent ability of NOD MΦs to autonomously shed VTCN1. Furthermore, the similar decline in VTCN1 levels was observed in B6^{g7}-originated MΦs from B6^{g7}→NOD-EGFP chimeras, indicating that non-hematopoietic cells of NOD mice induce strong acceleration of VTCN1 loss from B6^{g7}-derived cells. Interestingly, mRNA analysis showed increased *VTCN1* expression only in MΦs maturing in cellular environment of NOD, but not of B6^{g7} BM recipients (Fig. 5C, *left panel*), pointing towards up-regulation of *VTCN1* transcription as a likely compensatory feedback mechanism activated in response to strong systemic induction of VTCN1 loss. Finally, analysis of *NRD1* expression, which was found to be elevated in MΦs from chimeric animals harboring any NOD component (either hematopoietic or non-

hematopoietic; Fig. 5C, *right panel*), allowed us to conclude that: 1) augmentation of NRD1 expression is the characteristic trait of T1D-succeptible NOD background; 2) NRD1 is the likeliest candidate for the sought-after systemic VTCN1-destabilizing factor; and 3) the increased NRD1-mediated shedding is the major cause of VTCN1 decline observed in both MΦs and islet cells in conjunction with T1D development (Fig. 6).

Discussion

VTCN1 was identified as a negative co-stimulatory molecule with primary function of down-regulating immune responses by reducing T cell proliferation and cytokine production (5-7). *VTCN1* gene expression is not limited to APCs, but also occurs in several peripheral non-lymphoid tissues. Therefore, in addition to backing the anergic state of naïve T cells populating lymphatic organs (41), VTCN1-induced signaling can also negatively modulate already stimulated T cells, contributing to induction of peripheral tolerance (21, 42). Such a variety of expression patterns and functional activities suggests that VTCN1 plays a far more important role in the regulation of immune response than was previously appreciated.

Defective VTCN1 expression and/or presentation was coupled with exacerbation of several autoimmune diseases harboring hyper-activation of autoreactive T cells, namely T1D, RA, and multiple sclerosis (8, 9, 21, 43). Moreover, the delineation of defective VTCN1 presentation in RA-associated autoimmunity was directly related to the destruction of cell-associated VTCN1 and release of soluble VTCN1 (sVTCN1) fragments into the periphery (8). Extending these studies into the context of experimental and natural T1D, we recently demonstrated that high blood sVTCN1 concentrations in NOD mice and T1D patients are accompanied by almost complete loss of VTCN1 from the APCs' membranes (22). Based on these results, we suggested that sVTCN1 may serve as an early marker of clinical T1D in pediatric patients.

In contrast to the autoimmunity, VTCN1 levels on tumor cells and tumor-infiltrating APCs were found to be elevated in multiple neoplasms, providing for hypo-active anti-tumor T cell responses (44-47). Interestingly, such augmentation of VTCN1 in context of cancer development was also combined with elevated peripheral blood sVTCN1, which was proposed as a potential prognostic marker for metastatic cancer spread and consequent poor outcome in cancer patients (19, 48). It seems, however, that such a similar “high sVTCN1” phenotype is a result of different mechanisms governing VTCN1 metabolism with opposite outcomes – inhibited T cell responses in cancer or hyper-activated ones in autoimmunity.

Since VTCN1 was found to be expressed in the endocrine pancreas (9, 15, 21), we started this study with an intent to examine the functionality of endogenous VTCN1 in islet cells during T1D development, and to assess the natural VTCN1 capability to modulate autoimmune processes. We show that defective VTCN1 presentation from pancreatic islets, due to an increased shedding, precedes T1D development (Fig. 1). Surprisingly, despite the observed difference in the expression patterns between mice and humans, both α and β cells were found to be VTCN1-positive (Fig. S1). The drastic decrease of cell-associated VTCN1 levels detected in islets of human T1D patients was not limited to β cells, but surprisingly, affected several endocrine cell types (Fig. S1C), suggesting the presence of a general defect

in VTCN1 presentation. Moreover, the fact that VTCN1 loss in islets occurred despite elevated *VTCN1* mRNA expression (Fig. 1B – C) indicates the involvement of post-translational control mechanisms, such as protein degradation and/or shedding, in regulation of this process. Importantly, similarly to the islets, elevated *VTCN1* gene expression was also unable to compensate VTCN1 protein loss in MΦs from T1D-prone animals and human T1D patients [Fig. 5 B – C and (22)]. Taken together, these observations suggest that a general proteolytic mechanism responsible for defective VTCN1 presentation on multiple cell types is tied with the initiation and/or progression of diabetogenic autoimmunity (Fig. 6).

Accordingly, we suggested the metalloproteinase NRD1 as the common VTCN1-shedding enzyme responsible for impaired VTCN1 presentation in multiple tissues (Fig. 6). Stabilization of VTCN1 by NRD1 inhibitors in isolated islets (Fig. 2A), supplemented by the involvement of NRD1 proteinase in VTCN1 proteolysis in MΦs during T1D progression (22), clearly validates this suggestion. Moreover, application of the NRD1 inhibitor bestatin *ex vivo* restored the functionality of endogenous VTCN1 on NOD islets, as evidenced from the decreased proliferation and cytokine production of G9C8 $CD8^+$ T cells and BDC12-4.1 $CD4^+$ cells (Fig. 2D) in co-culturing experiments (Fig. 2B – D). These results evidently stressed the importance of endogenous VTCN1 presentation on both intra-islet APCs, and β cells for the local control of autoimmunity. In agreement, several studies have also showed that *ex vivo VTCN1* over-expression protects islet transplants/β cells from allograft rejection (20, 42, 49, 50). Though, our results indicate that *VTCN1* overexpression by itself will not address the shedding-dependent loss of functional VTCN1 protein. Therefore, development of better and more specific inhibitors of NRD1-directed VTCN1 proteolysis, as well as design of VTCN1-stabilizing agents of different nature, should be an important direction for future studies. This conclusion is in complete agreement with the observed partially-protective anti-diabetic effects of continuous bestatin administration to NOD mice, which alleviated, to the certain extent, autoimmune responses *via* systemic decrease of NRD1 activity (Fig. 3).

Further extending our findings of endogenous VTCN1 down-regulating anti-islet diabetogenic responses into an *in vivo* setting, we demonstrated that the proliferation of islet antigen-reactive T cells within insulitic lesions reversely correlated with the levels of VTCN1 presented by the islet cells (Fig. 4C – D). This result is consistent with the previous observations that *VTCN1* overexpression is protective against immune responses in two different systems: allograft survival of pancreatic islet transplants (20, 42) and in AI4αβ/B6.H2^{g7} severe diabetes mouse model (21). Moreover, the inflammatory influence of massive multi-cell insulitis, which is widely accepted to be the source of cytokines, growth factors, and other stimuli driving proliferation of diabetogenic T cells within islet infiltrates, was trumped by VTCN1-mediated inhibitory signaling, as intra-infiltrate T cells proliferated significantly better in low-VTCN1 presenting NOD islets, in comparison to high-VTCN1 B6^{g7} islets (Fig. 4D). Therefore, the intra-islet co-inhibition, delivered by proteolysis-uncompromised endogenous VTCN1, serves as a powerful local mechanism for self-protection against diabetogenicity.

Contrary to the common expectations, our adoptive transfer experiments demonstrated that stability of VTCN1 protein on islet cells was independent from accumulation of peri-islet lymphoid infiltrates. VTCN1 levels were steadily high in heavily infiltrated islets of B6^{g7} animals, while displaying a gradual age-dependent decline in the infiltrate-free islets of NOD-*scid* mice (Fig. 4A – C). Hence, VTCN1 degradation originates at least in part within the islet cells of diabetes-prone animals being therefore a cell-autonomous process characteristic for T1D-prone NOD background.

A more detailed investigation into the balance of VTCN1 loss, however, revealed that long-term engraftment of NOD BM cells into B6^{g7} hosts jeopardized islet VTCN1 levels through an extrinsic, systemic mechanism (Fig. 5A). Additionally, non-hematopoietic NOD cellular "environment" also induced accelerated VTCN1 loss in B6^{g7} BM-originated MΦs (Fig. 5B). Taken together, these data demonstrate that the persistent phenomenon of proteolytic impairment of functional VTCN1 presentation, detected in multiple cell types in conjunction with T1D-susceptibility, is regulated in two synergistically acting manners: cell-autonomous and systemic. The metalloproteinase NRD1, which has been found in several cell types including pancreatic islets (Fig 1C, D) and immune cells (Fig. 5C), where its activity is reported to be required for antigen processing and generation of cytotoxic T-lymphocyte epitopes (51), appear to fit both these modes. NRD1 protein is mainly localized in the cytosol but a significant proportion of the active enzyme is secreted through an unconventional secretory pathway and distributed on the cell surface (23). In agreement, our experimental data show up-regulation of *NRD1* gene expression in islets of diabetes-prone NOD mice (Fig. 1C), as well as in MΦs from BM-chimeric animals harboring any NOD component (Fig. 5C). Moreover, elevation of *NRD1* mRNA was accompanied by a gradual increase of NRD1 protein secretion from NOD islets, which paralleled the progression of T1D (Fig. 1D). Therefore, NRD1 is the likeliest constituent to deliver both cell-intrinsic VTCN1 ablation (through its intra-cellular activity) and systemic extrinsic VTCN1 loss (by its proteolytic actions in an extracellular, secreted mode). In summary, our results open the door for new studies addressing an important quest to identify the genetic and environmental factors responsible for up-regulation of NRD1 expression and enzymatic activity with respect to autoimmunity in general, and T1D in particular. Our current and previous findings strongly indicate that such factors are shared between autoimmunity-prone NOD mice and a substantial cluster of T1D patients. The elevated serum sVTCN1 levels (8) combined with an increased PBMCs' *NRD1* expression in RA patients (52), provide an initial insight into this quest, and hint that NRD1-dependent impairment of VTCN1-mediated negative co-stimulation is a general autoimmunity-associated pathway. In agreement, systemic NRD1 deficiency was recently reported to significantly reduce liver inflammation and protect mice from diet-induced nonalcoholic steatohepatitis (53). Our results imply a possibility that stabilization of VTCN1 in liver cells of these mice is a conceivable explanation for such a phenotype.

Interestingly, VTCN1 seems to mimic another endogenous mechanism of β cell protection, namely the PD-1/PD-L1 pathway. It has previously been shown that double-deficient for PD-L1 and PD-L2 NOD mice as well as PD-1 deficient animals, developed accelerated diabetes with 100% penetrance in both male and female mice (4, 54). In light of these

studies, the generation of VTCN1-knockout mice on the NOD background would be an interesting future direction that would provide us with valuable information about the VTCN1 importance in diabetes development in comparison to PD-1/PD-L1 pathway. Nevertheless, the existence of such redundancy in the negative co-stimulation signals on the periphery might be crucial for providing a multiple levels of defense of pancreatic islets against autoimmune destruction.

Our current data have multiple implications for a variety of disease conditions. For example, contrary to T1D, characterized by strong VTCN1 diminishment from the surface of multiple cell types, in several cancers VTCN1 shedding is not associated with loss, but rather with an increase of membrane-tethered VTCN1. Possible explanations could include an intra-tumor loss/down-regulation of NRD1 expression/activity or an over-compensatory excessive *VTCN1* expression. Subsequently, the control of NRD1 functionality appears to be a very attractive target for future investigations aimed at the development of novel therapeutics against either certain cancers or autoimmune conditions. Finally, our data shows that disrupted control of co-stimulation, evidenced by VTCN1 loss in both APCs and pancreatic islets, ultimately results in altered balance of control of immune responses.

Supplementary Material

Refer to Web version on PubMed Central for supplementary material.

Acknowledgments

We thank Drs. A. Chervonsky and V. Varnasi (Department of Pathology, The University of Chicago) for the transgenic B6.G9C8 mice. Authors are also grateful to Mr. Brady Roby for critical editing of manuscript and to Drs. Satoshi Nagata and Tomoko Ise (all Sanford Research) for helpful discussions. We are deeply thankful to staff of South Dakota Lions Eye and Tissue Bank for help with human tissue specimens' collection.

This work was supported by the Sanford Research start-up funds, JDRF research grant 47-2013-522 and NIH UC4 DK104194 subcontract, all to AYS. Support was also received by Sanford Research's Imaging and Flow Cytometry core facilities funded by the NIH COBRE grant 1P20RR024219.

References

1. Tisch R, McDevitt H. Insulin-dependent diabetes mellitus. Cell. 1996; 85:291–297. [PubMed: 8616883]
2. Velthuis JH, Unger WW, Abreu JR, Duinkerken G, Franken K, Peakman M, Bakker AH, Reker-Hadrup S, Keymeulen B, Drijfhout JW, Schumacher TN, Roep BO. Simultaneous detection of circulating autoreactive CD8+ T-cells specific for different islet cell-associated epitopes using combinatorial MHC multimers. Diabetes. 2010; 59:1721–1730. [PubMed: 20357361]
3. Ansari MJ, Salama AD, Chitnis T, Smith RN, Yagita H, Akiba H, Yamazaki T, Azuma M, Iwai H, Khoury SJ, Auchincloss H Jr, Sayegh MH. The programmed death-1 (PD-1) pathway regulates autoimmune diabetes in nonobese diabetic (NOD) mice. J Exp Med. 2003; 198:63–69. [PubMed: 12847137]
4. Wang J, Yoshida T, Nakaki F, Hiai H, Okazaki T, Honjo T. Establishment of NOD-Pdcd1-/- mice as an efficient animal model of type I diabetes. Proceedings of the National Academy of Sciences of the United States of America. 2005; 102:11823–11828. [PubMed: 16087865]
5. Prasad DV, Richards S, Mai XM, Dong C. B7S1, a novel B7 family member that negatively regulates T cell activation. Immunity. 2003; 18:863–873. [PubMed: 12818166]

6. Sica GL, Choi IH, Zhu G, Tamada K, Wang SD, Tamura H, Chapoval AI, Flies DB, Bajorath J, Chen L. B7-H4, a molecule of the B7 family, negatively regulates T cell immunity. Immunity. 2003; 18:849–861. [PubMed: 12818165]
7. Zang X, Loke P, Kim J, Murphy K, Waitz R, Allison JP. B7x: a widely expressed B7 family member that inhibits T cell activation. Proceedings of the National Academy of Sciences of the United States of America. 2003; 100:10388–10392. [PubMed: 12920180]
8. Azuma T, Zhu G, Xu H, Rietz AC, Drake CG, Matteson EL, Chen L. Potential role of decoy B7-H4 in the pathogenesis of rheumatoid arthritis: a mouse model informed by clinical data. PLoS medicine. 2009; 6:e1000166. [PubMed: 19841745]
9. Wei J, Loke P, Zang X, Allison JP. Tissue-specific expression of B7x protects from CD4 T cell-mediated autoimmunity. J Exp Med. 2011; 208:1683–1694. [PubMed: 21727190]
10. Wang X, Hao J, Metzger DL, Mui A, Ao Z, Akhoundsadegh N, Langermann S, Liu L, Chen L, Ou D, Verchere CB, Warnock GL. Early treatment of NOD mice with B7-H4 reduces the incidence of autoimmune diabetes. Diabetes. 2011; 60:3246–3255. [PubMed: 21984581]
11. Schwartz RH. Costimulation of T lymphocytes: the role of CD28, CTLA-4, and B7/BB1 in interleukin-2 production and immunotherapy. Cell. 1992; 71:1065–1068. [PubMed: 1335362]
12. Lu P, Wang YL, Linsley PS. Regulation of self-tolerance by CD80/CD86 interactions. Current opinion in immunology. 1997; 9:858–862. [PubMed: 9492990]
13. Choi IH, Zhu G, Sica GL, Strome SE, Cheville JC, Lau JS, Zhu Y, Flies DB, Tamada K, Chen L. Genomic organization and expression analysis of B7-H4, an immune inhibitory molecule of the B7 family. Journal of immunology. 2003; 171:4650–4654.
14. Ou D, Wang X, Metzger DL, Ao Z, Pozzilli P, James RF, Chen L, Warnock GL. Suppression of human T-cell responses to beta-cells by activation of B7-H4 pathway. Cell transplantation. 2006; 15:399–410. [PubMed: 16970282]
15. Cheung SS, Ou D, Metzger DL, Meloche M, Ao Z, Ng SS, Owen D, Warnock GL. B7-H4 expression in normal and diseased human islet beta cells. Pancreas. 2014; 43:128–134. [PubMed: 24326367]
16. Quandt D, Fiedler E, Boettcher D, Marsch W, Seliger B. B7-h4 expression in human melanoma: its association with patients' survival and antitumor immune response. Clin Cancer Res. 2011; 17:3100–3111. [PubMed: 21378130]
17. Sun Y, Wang Y, Zhao J, Gu M, Giscombe R, Lefvert AK, Wang X. B7-H3 and B7-H4 expression in non-small-cell lung cancer. Lung Cancer. 2006; 53:143–151. [PubMed: 16782226]
18. Zang X, Thompson RH, Al-Ahmadie HA, Serio AM, Reuter VE, Eastham JA, Scardino PT, Sharma P, Allison JP. B7-H3 and B7x are highly expressed in human prostate cancer and associated with disease spread and poor outcome. Proceedings of the National Academy of Sciences of the United States of America. 2007; 104:19458–19463. [PubMed: 18042703]
19. He C, Qiao H, Jiang H, Sun X. The inhibitory role of b7-h4 in antitumor immunity: association with cancer progression and survival. Clin Dev Immunol. 2011; 2011:695834. [PubMed: 22013483]
20. Wang X, Hao J, Metzger DL, Mui A, Ao Z, Verchere CB, Chen L, Ou D, Warnock GL. Local expression of B7-H4 by recombinant adenovirus transduction in mouse islets prolongs allograft survival. Transplantation. 2009; 87:482–490. [PubMed: 19307783]
21. Lee JS, Scandiuzzi L, Ray A, Wei J, Hofmeyer KA, Abadi YM, Loke P, Lin J, Yuan J, Serreze DV, Allison JP, Zang X. B7x in the Periphery Abrogates Pancreas-Specific Damage Mediated by Self-reactive CD8 T Cells. Journal of immunology. 2012; 189:4165–4174.
22. Radichev IA, Maneva-Radicheva LV, Amatya C, Parker C, Ellefson J, Wasserfall C, Atkinson M, Burn P, Savinov AY. Nardilysin-Dependent Proteolysis of Cell-Associated VTCN1 (B7-H4) Marks Type 1 Diabetes Development. Diabetes. 2014; 63:3470–3482. [PubMed: 24848066]
23. Hospital V, Chesneau V, Balogh A, Joulie C, Seidah NG, Cohen P, Prat A. N-arginine dibasic convertase (nardilysin) isoforms are soluble dibasic-specific metalloendopeptidases that localize in the cytoplasm and at the cell surface. The Biochemical journal. 2000; 349:587–597. [PubMed: 10880358]
24. Seidah NG, Prat A. Precursor convertases in the secretory pathway, cytosol and extracellular milieu. Essays in biochemistry. 2002; 38:79–94. [PubMed: 12463163]

25. Varanasi V, Avanesyan L, Schumann DM, Chervonsky AV. Cytotoxic Mechanisms Employed by Mouse T Cells to Destroy Pancreatic beta-Cells. Diabetes. 2012
26. Savinov AY, Wong FS, Chervonsky AV. IFN-gamma affects homing of diabetogenic T cells. Journal of immunology. 2001; 167:6637–6643.
27. Chen YG, Silveira PA, Osborne MA, Chapman HD, Serreze DV. Cellular expression requirements for inhibition of type 1 diabetes by a dominantly protective major histocompatibility complex haplotype. Diabetes. 2007; 56:424–430. [PubMed: 17259387]
28. Szot GL, Koudria P, Bluestone JA. Murine pancreatic islet isolation. J Vis Exp. 2007:255. [PubMed: 18989427]
29. Maneva-Radicheva L, Amatya C, Parker C, Ellefson J, Radichev I, Raghavan A, Charles ML, Williams MS, Robbins MS, Savinov AY. Autoimmune diabetes is suppressed by treatment with recombinant human tissue Kallikrein-1. PLoS One. 2014; 9:e107213. [PubMed: 25259810]
30. Csuhai E, Safavi A, Hersh LB. Purification and characterization of a secreted arginine-specific dibasic cleaving enzyme from EL-4 cells. Biochemistry. 1995; 34:12411–12419. [PubMed: 7547986]
31. Chesneau V, Pierotti AR, Barre N, Creminon C, Tougard C, Cohen P. Isolation and characterization of a dibasic selective metalloendopeptidase from rat testes that cleaves at the amino terminus of arginine residues. J Biol Chem. 1994; 269:2056–2061. [PubMed: 8294457]
32. Foulon T, Cadel S, Chesneau V, Draoui M, Prat A, Cohen P. Two novel metallopeptidases with a specificity for basic residues: functional properties, structure and cellular distribution. Ann N Y Acad Sci. 1996; 780:106–120. [PubMed: 8602724]
33. Wong FS, Karttunen J, Dumont C, Wen L, Visintin I, Pilip IM, Shastri N, Pamer EG, Janeway CA Jr. Identification of an MHC class I-restricted autoantigen in type 1 diabetes by screening an organ-specific cDNA library. Nature medicine. 1999; 5:1026–1031.
34. Jasinski JM, Yu L, Nakayama M, Li MM, Lipes MA, Eisenbarth GS, Liu E. Transgenic insulin (B: 9-23) T-cell receptor mice develop autoimmune diabetes dependent upon RAG genotype, H-2g7 homozygosity, and insulin 2 gene knockout. Diabetes. 2006; 55:1978–1984. [PubMed: 16804066]
35. Moore A, Grimm J, Han B, Santamaria P. Tracking the recruitment of diabetogenic CD8+ T-cells to the pancreas in real time. Diabetes. 2004; 53:1459–1466. [PubMed: 15161749]
36. Podojil JR, Liu LN, Marshall SA, Chiang MY, Goings GE, Chen L, Langermann S, Miller SD. B7-H4Ig inhibits mouse and human T-cell function and treats EAE via IL-10/Treg-dependent mechanisms. Journal of autoimmunity. 2013; 44:71–81. [PubMed: 23683881]
37. Eizirik DL, Colli ML, Ortis F. The role of inflammation in insulitis and beta-cell loss in type 1 diabetes. Nature reviews Endocrinology. 2009; 5:219–226.
38. Martinuzzi E, Lemonnier FA, Boitard C, Mallone R. Measurement of CD8 T cell responses in human type 1 diabetes. Ann N Y Acad Sci. 2008; 1150:61–67. [PubMed: 19120269]
39. Roep BO. T-cell responses to autoantigens in IDDM. The search for the Holy Grail. Diabetes. 1996; 45:1147–1156. [PubMed: 8772714]
40. Shultz LD, Schweitzer PA, Christianson SW, Gott B, Schweitzer IB, Tennent B, McKenna S, Mobraaten L, Rajan TV, Greiner DL, et al. Multiple defects in innate and adaptive immunologic function in NOD/LtSz-scid mice. Journal of immunology. 1995; 154:180–191.
41. Kryczek I, Wei S, Zou L, Zhu G, Mottram P, Xu H, Chen L, Zou W. Cutting edge: induction of B7-H4 on APCs through IL-10 novel suppressive model for regulatory T cells. Journal of immunology. 2006; 177:40–44.
42. Wang X, Hao J, Metzger DL, Mui A, Ao Z, Verchere CB, Chen L, Ou D, Warnock GL. B7-H4 induces donor-specific tolerance in mouse islet allografts. Cell transplantation. 2012; 21:99–111. [PubMed: 21929869]
43. Chen L, Lu Y, Wang F, Zhou M, Chu Y, Ding W, Liu C, Xie J, Wu C, Jiang J. Expression of co-stimulatory molecule B7-H4 in patients suffering from rheumatoid arthritis. Immunology letters. 2013; 154:25–30. [PubMed: 23973734]
44. Chen C, Qu QX, Shen Y, Mu CY, Zhu YB, Zhang XG, Huang JA. Induced expression of B7-H4 on the surface of lung cancer cell by the tumor-associated macrophages: a potential mechanism of immune escape. Cancer letters. 2012; 317:99–105. [PubMed: 22108530]

45. Ichikawa M, Chen L. Role of B7-H1 and B7-H4 molecules in down-regulating effector phase of T-cell immunity: novel cancer escaping mechanisms. Frontiers in bioscience : a journal and virtual library. 2005; 10:2856–2860. [PubMed: 15970540]
46. Krambeck AE, Thompson RH, Dong H, Lohse CM, Park ES, Kuntz SM, Leibovich BC, Blute ML, Cheville JC, Kwon ED. B7-H4 expression in renal cell carcinoma and tumor vasculature: associations with cancer progression and survival. Proceedings of the National Academy of Sciences of the United States of America. 2006; 103:10391–10396. [PubMed: 16798883]
47. Kryczek I, Zou L, Rodriguez P, Zhu G, Wei S, Mottram P, Brumlik M, Cheng P, Curiel T, Myers L, Lackner A, Alvarez X, Ochoa A, Chen L, Zou W. B7-H4 expression identifies a novel suppressive macrophage population in human ovarian carcinoma. J Exp Med. 2006; 203:871–881. [PubMed: 16606666]
48. Shi H, Ji M, Wu J, Zhou Q, Li X, Li Z, Zheng X, Xu B, Zhao W, Wu C, Jiang J. Serum B7-H4 expression is a significant prognostic indicator for patients with gastric cancer. World journal of surgical oncology. 2014; 12:188. [PubMed: 24947047]
49. Yuan CL, Xu JF, Tong J, Yang H, He FR, Gong Q, Xiong P, Duan L, Fang M, Tan Z, Xu Y, Chen YF, Zheng F, Gong FL. B7-H4 transfection prolongs beta-cell graft survival. Transpl Immunol. 2009; 21:143–149. [PubMed: 19361556]
50. Wang X, Hao J, Metzger DL, Mui A, Lee IF, Akhoundsadegh N, Chen CL, Ou D, Ao Z, Verchere CB, Warnock GL. Blockade of both B7-H4 and CTLA-4 co-signaling pathways enhances mouse islet allograft survival. Islets. 2012; 4:284–295. [PubMed: 22878670]
51. Kessler JH, Khan S, Seifert U, Le Gall S, Chow KM, Paschen A, Bres-Vloemans SA, de Ru A, van Montfoort N, Franken KL, Benckhuijsen WE, Brooks JM, van Hall T, Ray K, Mulder A, Doxiadis II, van Swieten PF, Overkleeft HS, Prat A, Tomkinson B, Neefjes J, Kloetzel PM, Rodgers DW, Hersh LB, Drijfhout JW, van Veelen PA, Ossendorp F, Melief CJ. Antigen processing by nardilysin and thimet oligopeptidase generates cytotoxic T cell epitopes. Nat Immunol. 2011; 12:45–53. [PubMed: 21151101]
52. Teixeira VH, Olaso R, Martin-Magniette ML, Lasbleiz S, Jacq L, Oliveira CR, Hilliquin P, Gut I, Cornelis F, Petit-Teixeira E. Transcriptome analysis describing new immunity and defense genes in peripheral blood mononuclear cells of rheumatoid arthritis patients. PLoS One. 2009; 4:e6803. [PubMed: 19710928]
53. Ishizu-Higashi S, Seno H, Nishi E, Matsumoto Y, Ikuta K, Tsuda M, Kimura Y, Takada Y, Kimura Y, Nakanishi Y, Kanda K, Komekado H, Chiba T. Deletion of nardilysin prevents the development of steatohepatitis and liver fibrotic changes. PLoS One. 2014; 9:e98017. [PubMed: 24849253]
54. Keir ME, Liang SC, Guleria I, Latchman YE, Qipo A, Albacker LA, Koulmanda M, Freeman GJ, Sayegh MH, Sharpe AH. Tissue expression of PD-L1 mediates peripheral T cell tolerance. J Exp Med. 2006; 203:883–895. [PubMed: 16606670]

Abbreviations

VTCN1	V-set domain-containing T cell activation inhibitor-1
sVTCN1	soluble VTCN1
NRD1	N-arginine dibasic convertase 1
PD-1/PD-L1	Programmed cell death-1 protein/Programmed cell death-ligand 1
PCSK1/2	proprotein convertase subtilisin/kexin type 1/2
BM	bone marrow
MΦ	macrophage
Tregs	T regulatory cells

T1D	type 1 diabetes
RA	rheumatoid arthritis
EdU	5-ethynyl-2′-deoxyuridine
RFU	Relative fluorescence units

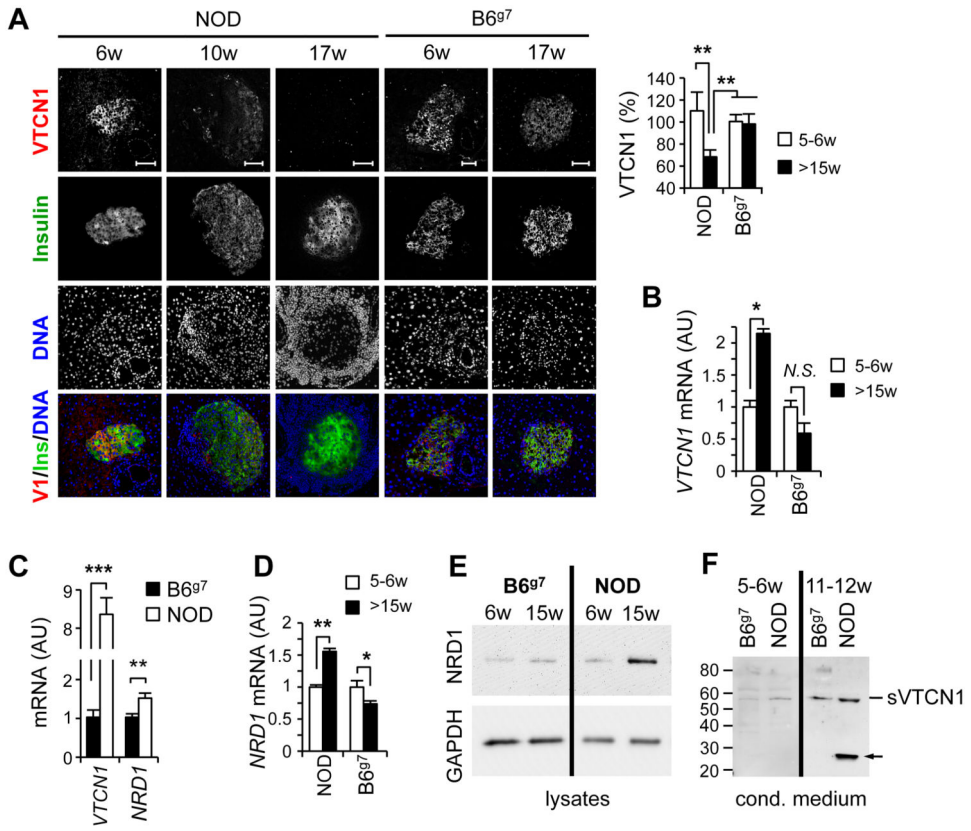

Figure 1. T1D development is accompanied by the proteolytic decrease of VTCN1 protein on islets cells

(A) Age-related decline of VTCN1-immunoreactivity in NOD islets. Representative images (*left*) and quantitative analysis (*right*) of pancreatic cryosections from NOD and B6^{g7} mice of indicated ages stained for VTCN1 (red) and insulin (green). Data are expressed as a percentage of relative fluorescence units (RFU) when compared to islets from 5 week-old B6^{g7} mice (n=3- 5 mice/group) ±SEM. RFU were calculated for ≥20 individual islets/animal by subtracting mean control antibody fluorescence from mean test antibody fluorescence. Scale bars, 50 μm. ***p*<0.01 (**B**) RT-qPCR analysis of *VTCN1* mRNA (normalized to *GAPDH*) isolated from pooled islets (n=4-5 mice/group) from NOD mice at the indicated age. Data are shown as mean arbitrary units (AU) ±SEM. **p*<0.05. (**C**) Quantitative RT-qPCR analysis of *VTCN1* and *NRD1* mRNAs in pancreatic islets from NOD and B6^{g7} mice. Data are shown as the mean ±SEM (n=4-5 mice/group); ***p*<0.01; ****p*<0.001. (**D**) NRD1 immunoblot of lysates of islets isolated from B6^{g7} or NOD mice of indicated ages. (**E**) VTCN1 immunoblot of medium conditioned by islets isolated from NOD or B6^{g7} mice. Arrow indicates a possible degradation product of sVTCN1 observed in conditioned by NOD islets medium.

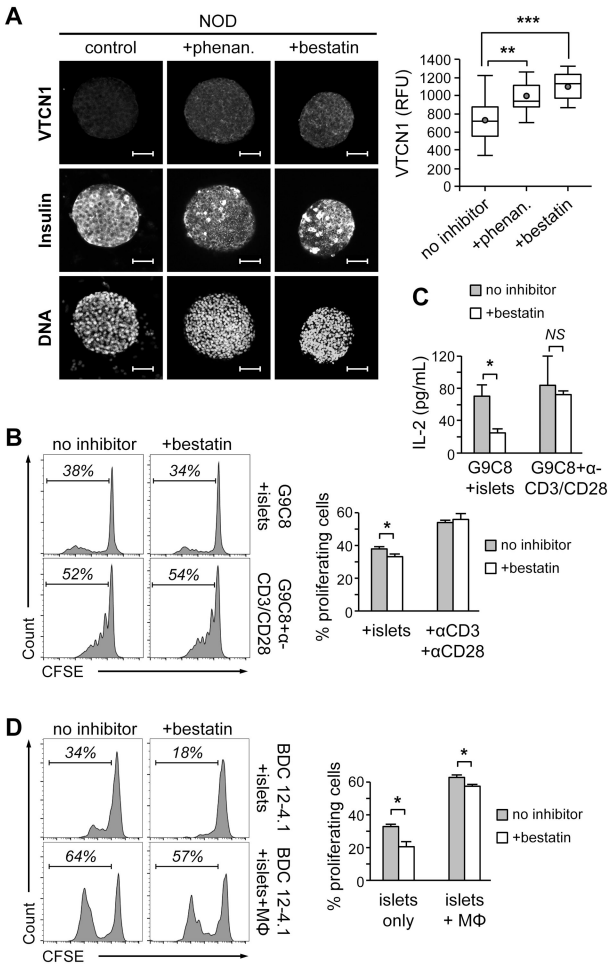

Figure 2. NRD1 inhibition improves surface localization and functionality of VTCN1

(**A**) Representative images (*left*) and quantitative analysis (*right*) of VTCN1 immunostaining of isolated whole NOD islets cultured for 24 hours with vehicle or with the indicated NRD1-inhibitor (n=30-40 islets, 3 mice per group). Red dots and the horizontal lines in each box indicate the mean and the median values, respectively; **p<0.01; ***p<0.001; Scale bars, 50 μm. (**B**) *Left histograms* – Flow cytometry analysis of 7-AAD-negative CFSE-labeled G9C8 cells co-cultured for 5 days with dispersed NOD islets or anti-CD3/anti-CD28 beads in the presence or absence of 10 μM bestatin. *Right graph* – percentage of G9C8 proliferating cells; *p<0.05. (**C**) Conditioned medium collected after 3 days of G9C8 cells/ islet cells co-cultures of as in (**B**) was analyzed by ELISA for IL-2 concentrations. (**D**) *Left histograms* – Flow cytometry analysis of 7-AAD-negative CFSE-labeled BDC12-4.1 $CD4^+$ T cells co-cultured for 5 days with dispersed NOD islets only (*top panels*) or dispersed islets and MΦs (*lower panels*) in the presence or absence of 10 μM bestatin. *Right graphs* – percentage of BDC12-4.1 proliferating cells; *p<0.05. **B-D** n=5-6.

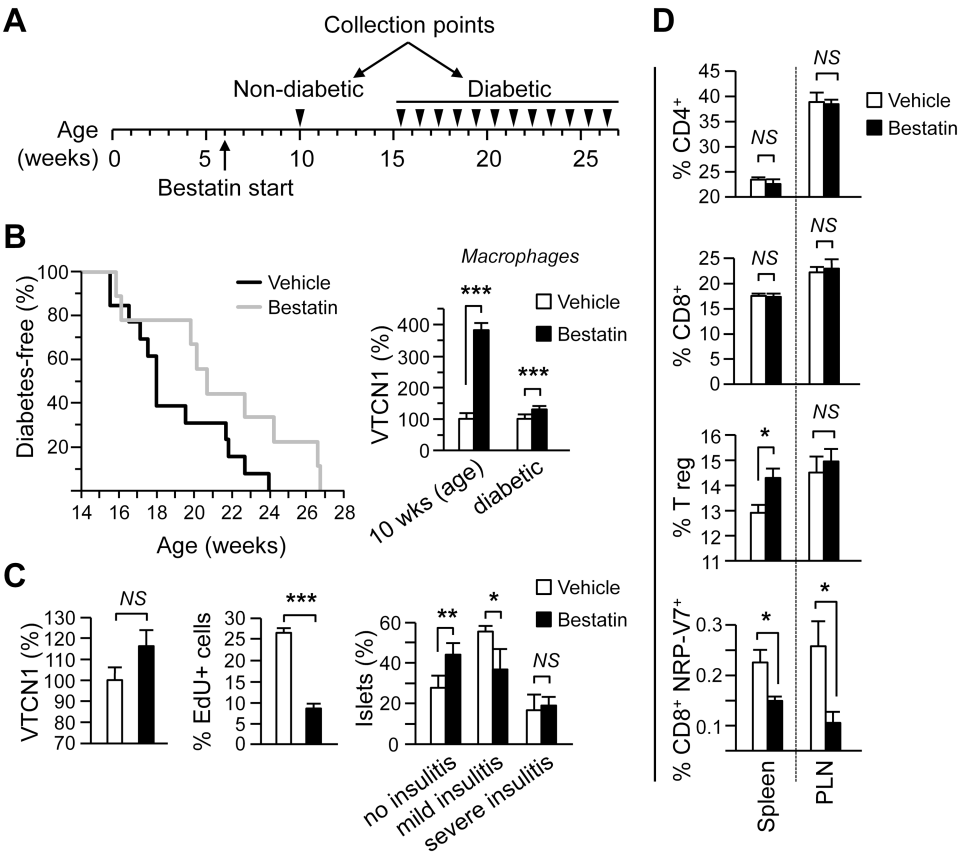

Figure 3. Limited tolerance-promoting effects of systemic bestatin administration to NOD mice

(**A**) Schematic representation of treatment regimen. (**B**). *Left* – Spontaneous T1D incidence in NOD female mice continuously treated from 6 weeks of age with daily *i.p.* injections of bestatin (n=12 *grey line*) or vehicle (n=14 *black line*). Difference in incidence ($p<0.05$) was analyzed using Log-rank survival curve analysis. *Right* – Peritoneal MΦs from mice treated for 4 weeks (n=7-mice/group) or until diabetes development (n=12-14 mice/group) were fixed, stained for membrane VTCN1 and analyzed by immunofluorescence. The relative surface VTCN1 fluorescence of MΦs from bestatin-treated mice is plotted as a percentage from the vehicle-treated control animals. (**C**). Pancreatic sections from treated for 4 weeks mice (n=7-mice/group) were stained for insulin and VTCN1 (*left*) or EdU (*middle*). The relative fluorescence of VTCN1 in pancreatic islets was measured and plotted as a percentage from the vehicle-treated controls. Insulitis score (*right*) was evaluated by grading in a blinded fashion as described in Materials and Methods. (**D**) Percentage of $CD4^+$, $CD8^+$, Tregs and NRP-$V7^+$ cells in spleens and PLNs isolated from bestatin- or vehicle-treated mice after 4 weeks of treatment (n=7-mice/group). Single cell suspensions were stained for either CD4/CD25/FoxP3 or CD8/NRP-V7 and then analyzed by FACS. *$p<0.05$; **$p<0.001$.

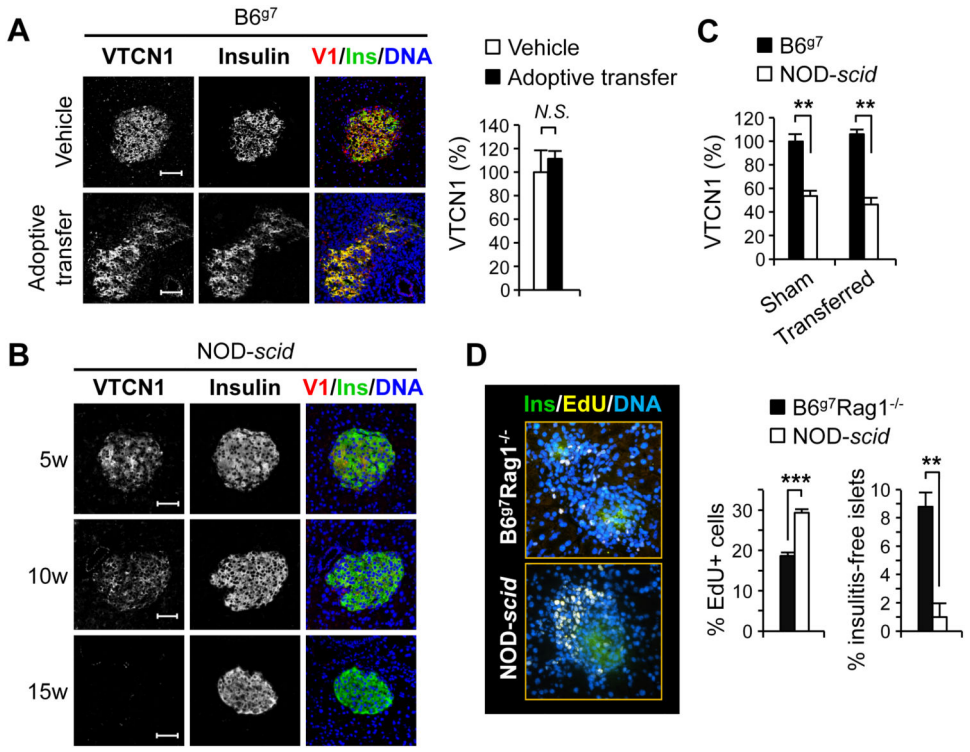

Figure 4. Autoimmunity is ameliorated by high levels of endogenous islet cells' VTCN1

(**A**) Representative immunofluorescent images (*left*) and quantitative analysis (*right*) of pancreatic islets from B6^{g7} mice 20 days after reception of 10^7 splenocytes from acutely diabetic NOD mouse (*Adoptive transfer*) or vehicle solution (*vehicle*) (n=3-5 mice/group). Overlay of VTCN1 (red), insulin (green), and DNA (blue) is shown in the third column. (**B**) Representative images of pancreatic cryosections from NOD-*scid* mice of indicated ages stained for VTCN1 (red) and insulin (green). (**C**) Changes in the VTCN1 immunoreactivity in islets from vehicle-transferred (*Sham*) or splenocytes-transferred (*Transferred*) NOD-*scid* and irradiated B6^{g7} mice 3 weeks after adoptive transfers of 10^7 splenocytes from acutely diabetic NOD mice (n=3-4 mice/group). (**D**) Representative images (*left*) and quantitative analysis (*right*) of EdU-positive T cells within insulitic lesions of adoptively transferred, as in C, NOD-*scid* and B6^{g7}-Rag1$^{-/-}$mice, 3 weeks after transfer (n=3-4 mice/group). Scale bars, 50 μm; **p<0.01, ***p<0.001.

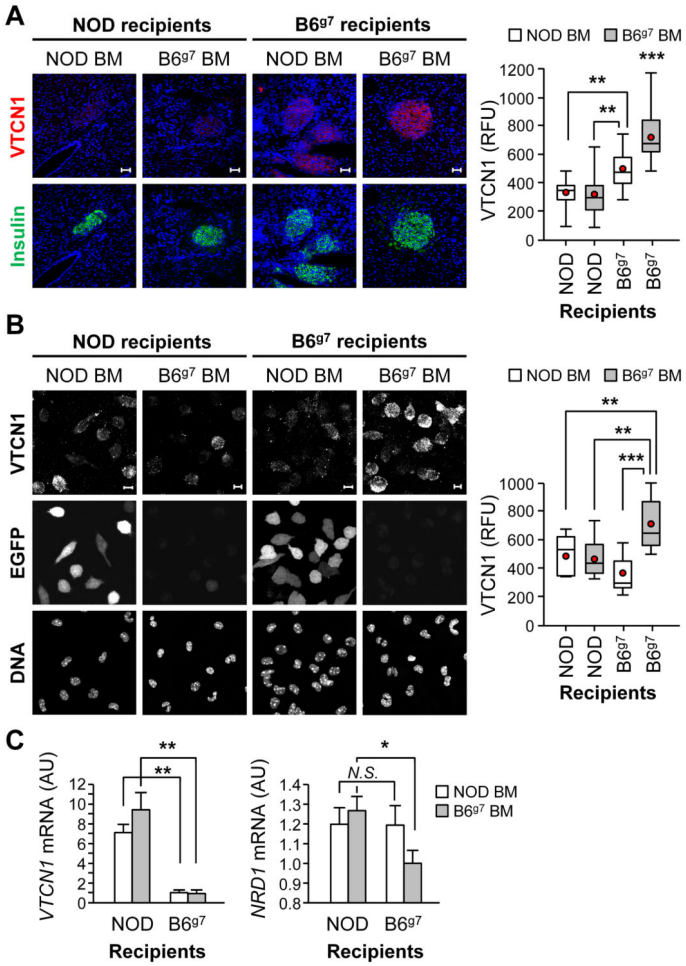

Figure 5. Cell-autonomous and systemic augmentation of NRD1, characteristic for diabetes-prone NOD mice, determines defective VTCN1 presentation in multiple cell types

(**A**) Representative images (*left*) and quantitative analysis (*right*) of pancreatic cryosections from NOD and B6^{g7} chimeric mice collected 10 weeks after the bone marrow transfer (n=3-4 mice/group). Scale bars, 50 μm. (**B**) Representative images (*left*) and quantitative analysis (*right*) of peritoneal MΦs isolated from NOD and B6^{g7} chimeric mice; Scale bars, 10 μm. **A, B** Red dots and the horizontal lines in each box indicate the mean and the median values, respectively. (**C**) RT-qPCR analysis of *VTCN1* (*left*) and *NRD1* (*right*) mRNAs in peritoneal MΦs isolated from NOD and B6^{g7} chimeric mice. The generated chimeras were: NOD-EGFP→NOD (NOD-EGFP donor into NOD recipient), B6^{g7}→NOD-EGFP (B6^{g7} donor into NOD-EGFP recipient), NOD-EGFP→B6^{g7} (NOD-EGFP donor into B6^{g7} recipient) and B6^{g7}→B6^{g7} (B6^{g7} donor into B6^{g7} recipient); *p<0.05; **p<0.01; ***p<0.001.

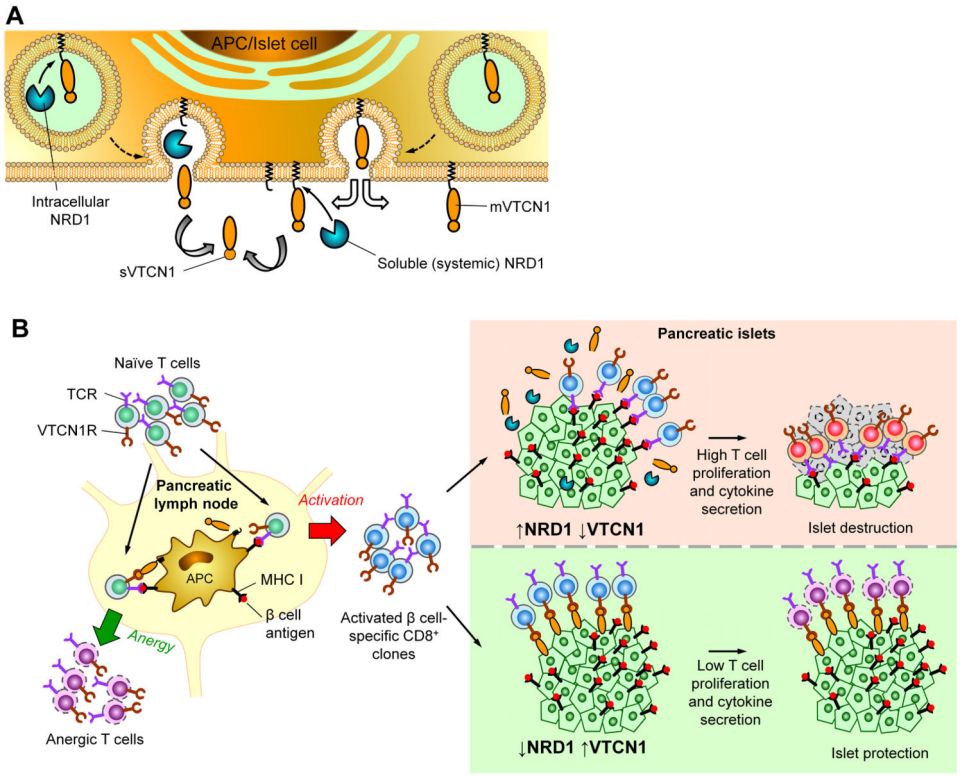

Figure 6. Schematic view of the impairment of VTCN1-dependent negative co-stimulation in context of T1D development

(**A**) Cell-intrinsic and -extrinsic modes of VTCN1/NRD1 interactions. Cells with low internal levels of NRD1 display uninterrupted presentation of full length VTCN1 tethered to the cell membrane (mVTCN1), while high intracellular NRD1 production results in VTCN1 proteolysis and generation of soluble VTCN1 (sVTCN1) fragments. NRD1, secreted from high-producing surrounding cells, compliment VTCN1 proteolysis acting extracellularly. (**B**) Function of NRD1/VTCN1 axis in the development of T1D. *Left*, outcome of antigen-specific activation of islet-eactive T cells by APCs in pancreatic lymph nodes depends on NRD1/VTCN1 interplay. Low levels of intracellular and systemic NRD1 allow the continuous presentation of functional membrane-tethered VTCN1 by APCs, which provides negative co-stimulatory signal anergizing autoreactive T cells. When high NRD1 levels are present VTCN1 is being cleaved, negative co-stimulation is abrogated, and hyper-activation of autoreactive T cells is induced. *Right*, activated β cell-specific T cells migrate toward pancreatic islets and accumulate in islet infiltrates, where two potential scenarios, depending on NRD1 levels, occur: 1) Low NRD1 content and consequent high mVTCN1 levels on islet cells are protective, as VTCN1 signalling reduces proliferation and cytokine production of accumulating T cells; 2) Absence of mVTCN1 on the islets cells due to an increased NRD1-mediated shedding results in hyper proliferation of autoreactive T cells and consequent β cell destruction. VTCN1R – putative VTCN1 receptor.